© 2017. Published by The Company of Biologists Ltd | Journal of Cell Science (2017) 130, 2808-2820 doi:10.1242/jcs.198903

RESEARCH ARTICLE

The ShcD phosphotyrosine adaptor subverts canonical EGF receptor trafficking

Melanie K. B. Wills, Hayley R. Lau and Nina Jones*

ABSTRACT

Shc family signalling adaptors connect activated transmembrane receptors to proximal effectors, and most also contain a sequence involved in clathrin-mediated receptor endocytosis. Notably, this AP2 adaptin-binding motif (AD) is absent from the ShcD (also known as Shc4) homolog, which also uniquely promotes ligand-independent phosphorylation of the epidermal growth factor receptor (EGFR). We now report that cultured cells expressing ShcD exhibit reduced EGF uptake, commensurate with a decrease in EGFR surface presentation. Under basal conditions, ShcD colocalises with the EGFR and facilitates its phosphorylation, ubiquitylation and accumulation in juxtanuclear vesicles identified as Rab11-positive endocytic recycling compartments. Accordingly, ShcD also functions as a constitutive binding partner for the E3 ubiquitin ligase Cbl. EGFR phosphorylation and focal accumulation likewise occur upon ShcD co-expression in U87 glioma cells. Loss of ShcD phosphotyrosine-binding function or insertion of the ShcA AD sequence each restore ligand acquisition through distinct mechanisms. The AD region also contains a nuclear export signal, indicating its multifunctionality. Overall, ShcD appears to possess several molecular permutations that actively govern the EGFR, which may have implications in development and disease.

KEY WORDS: Signal transduction, RTK endocytosis, ShcA, ShcD, EGFR, AP2, Clathrin-mediated endocytosis, NES, Ubiquitin, Cbl

INTRODUCTION

Proteins of the Src homology and collagen (Shc) family are best characterised as phosphotyrosine adaptors in signal transduction cascades. Accordingly, they are anchored at the N- and C-termini by a phosphotyrosine-binding (PTB) domain and Src homology 2 (SH2) domain, respectively, which enable the adaptors to engage recognition motifs on active transmembrane receptors. These domains bracket a central collagen homology 1 (CH1) region containing conserved tyrosine motifs that undergo stimulus-induced phosphorylation, thus converting the Shc protein into a scaffold (Wills and Jones, 2012).

Four members of the Shc family have been described in mammals, commonly designated ShcA, ShcB, ShcC and ShcD (or Shc1 through Shc4) in chronological order of their discovery. ShcA is the best characterised and most ubiquitously expressed, while ShcB, ShcC and ShcD primarily localise to nervous tissue and are less understood (Wills and Jones, 2012). Despite the conserved architecture and considerable amino acid identity between the respective PTB and SH2 domains of the four Shc proteins, distinct roles have been ascribed to the individual homologs and the unique protein isoforms therein (Jones et al., 2007; Wills and Jones, 2012). Structurally, ShcD is most similar to ShcA (Jones et al., 2007), although their level of functional overlap has yet to be determined.

ShcA has been studied extensively in the context of the epidermal growth factor receptor (EGFR), which serves as a classic model of receptor tyrosine kinase (RTK) signalling and endocytosis (Sorkin and Goh, 2009). EGFR is also of great biomedical significance as a mechanistic factor in many cancers (Cai et al., 2010). Proximal to the ligand-activated EGFR, ShcA becomes tyrosine phosphorylated in the CH1 region at consensus binding motifs for the Grb2 adaptor, which in turn initiates events in the Ras to mitogen-activated protein kinase (MAPK) cascade to augment the downstream activation of ERK1 and ERK2 (ERK1/2, also known as MAPK3 and MAPK1, respectively) (Migliaccio et al., 1997; Rozakis-Adcock et al., 1992; van der Geer et al., 1996; Wills and Jones, 2012).

Internalisation of the EGFR is a vital step in ligand-mediated transduction that has both informatic and regulatory functions. Endocytic vesicles remove engaged receptors from the cell surface, and provide a platform for a variety of signalling transactions (Murphy et al., 2009). The endocytosis machinery also determines the fate of the EGFR, either recycling it to the plasma membrane to intercept future stimuli, or relegating it to the lysosome for degradation. The predominant and best-characterised internalisation route is clathrin-mediated endocytosis (CME), which specifically removes cargo from the surface via pits and vesicles that are coated in a clathrin protein lattice (Goh and Sorkin, 2013). The destiny of the endocytosed EGFR is then determined by the pattern of receptor ubiquitylation, which in turn is orchestrated by the E3 ubiquitin (Ub) ligase, c-Cbl (henceforth designated Cbl), upon its recruitment to the signalling complex (Umebayashi et al., 2008). Traditionally considered a lysosome-directed tag, ubiquitin has a contested role in endocytosis as evidence continues to accrue that additionally implicates it as a fundamental trafficking mediator (Fortian et al., 2015).

Shc proteins are known to engage in the EGFR internalisation process due to a short sequence in the CH1 region that binds adaptin subunits of the adaptor protein 2 (AP2) complex (Okabayashi et al., 1996; Sakaguchi et al., 2001). AP2 is central to CME, specifically engaging in selection of cargo destined for internalisation, and linking it to the clathrin triskelia (McMahon and Boucrot, 2011). ShcA has been found to promote both AP2 recruitment to the receptor, as well as EGF uptake (Sakaguchi et al., 2001).

Intriguingly, the AP2 adaptin-binding motif (AD) is conserved across all Shc adaptors except ShcD, and the physiological consequence of this loss has not yet been investigated. We have previously shown that ShcD is an EGFR binding partner that possesses the unique capacity to promote ligand-independent

Department of Molecular and Cellular Biology, University of Guelph, Guelph, ON, N1G 2W1, Canada.

*Author for correspondence (jonesmcb@uoguelph.ca)

M.K.B.W., 0000-0002-7448-8657; N.J., 0000-0003-3382-5589

Received 26 October 2016; Accepted 9 July 2017

Journal of Cell Science

Journal of Cell Science (2017) 130, 2808-2820 doi:10.1242/jcs.198903

phosphorylation of the receptor on three physiologically relevant sites – Y1068, Y1148 and Y1173 (Wills et al., 2014). This phenomenon was found to require both the intrinsic EGFR kinase, and the PTB domain of ShcD. We now demonstrate that ShcD alters steady-state EGFR trafficking dynamics, which reduces cellular ligand sensitivity by recruiting the receptor into juxtanuclear endocytic recycling compartments where it is sheltered from external stimuli. Transplantation of the AD motif into ShcD helps to restore surface presentation of the receptor, and hence, ligand uptake. The EGFR is also highly ubiquitylated in the presence of ShcD, corresponding to our discovery of a constitutive ShcD–Cbl interaction.

Our findings further underscore the non-canonical characteristics of ShcD, which may be of particular relevance to the malignancies in which ShcD is overexpressed, including glioma (Wills et al., 2014) and melanoma (Fagiani et al., 2007).

RESULTS

ShcD expression reduces EGF uptake

Shc family proteins are established modulators of EGFR signalling, and the aforementioned atypical characteristics of ShcD prompted us to investigate its impact on EGF-induced receptor internalisation. To first compare the ligand response of ShcD to that of the closely related ShcA, we expressed GFP-tagged proteins in COS-1 cells, which possess robust levels of endogenous EGFR. Serum-starved cells were incubated at 4°C with fluorescently tagged EGF, rinsed, and warmed to 37°C to permit internalisation of receptor and bound ligand. Confocal microscopy was then used on fixed specimens to evaluate the presence and distribution of Shc and EGF.

As anticipated, ShcA-expressing cells formed visible EGF vesicles upon stimulation, and these puncta were found to colocalise extensively with ShcA (Fig. 1A, top row). Conversely, ShcD distribution was characterised by larger, more globular structures, often residing in the perinuclear space and excluding EGF (Fig. 1A, second row). Such cells were largely devoid of internalised EGF signal altogether, although weak staining was evident along the cellular peripheries. In contrast to both ShcA- and ShcD-expressing cells, control GFP transfectants displayed diffuse green fluorescence that did not align with EGF vesicles. To quantify this phenomenon, we processed cells by flow cytometry and determined the extent to which transfected cells acquired EGF. As depicted in Fig. 1B, ShcD cells demonstrated a significant reduction in the ligand signal as compared to that of ShcA and GFP. This supports the observations made at the level of individual cells that ShcD expression suppresses ligand uptake.

EGFR is sequestered in the cell with ShcD

We next sought to determine whether a reduced EGF response in the presence of ShcD might reflect altered EGFR dynamics at the cell surface. To characterise subcellular localisation, we simultaneously monitored ShcA–GFP or ShcD–GFP (depicted in blue), total and active EGFR (green), and EGF (red), in relation to the location of the nucleus (grey) (Fig. 2A). The phosphorylation status of EGFR residue Y1068, which is a major and immediate target of the intrinsic kinase and a primary Grb2-binding site (Tong et al., 2014), was used as a readout of receptor autophosphorylation, as previously described (Wills et al., 2014). Consistent with our findings from Fig. 1A, ShcA associated with vesicles that were positive for EGFR, phosphorylated (p)EGFR and EGF, which appear white in the composite images (Fig. 2A). These puncta were found to distribute uniformly throughout the cytoplasm. Also as anticipated, GFP alone was unresponsive to stimulus, and did not influence the distribution of receptor or ligand (Fig. 2A). By contrast, ShcD was again identified in perinuclear clusters that excluded EGF (Fig. 2A). Notably, however, the ShcD puncta were positive for both EGFR and pEGFR Y1068, which appears as cyan in the composite. The conspicuous absence of ligand in these vesicles implied that receptor localisation and phosphorylation were independent of exogenous EGF. To further investigate this observation, we focused on the serum-deprived basal state and verified that ShcD maintained its highly punctate distribution irrespective of growth factor treatment, and in stark contrast to the diffuse and uniform appearance of ShcA (Fig. 2B). To quantify the phenomenon, we classified unstimulated transfectants based on the extent of observable ShcD vesiculation, and found that 75.86% of cells exhibited a high degree of ShcD structure, similar to the pattern depicted in Fig. 2B (Fig. 2C). Moreover, when compared against ShcA and GFP alone, ShcD was confirmed to promote ligand-independent tyrosine phosphorylation of the EGFR (Fig. 2B, F), as we reported previously (Wills et al., 2014). Strikingly, this phospho-induction was only apparent in ShcD- and EGFR-positive puncta, which were enriched in the juxtanuclear space (Fig. 2B). EGFR remained unphosphorylated in the absence of ShcD vesicles, suggesting that the phenomena of receptor activation and focal accumulation are tightly correlated in this context.

Since all indications suggested that ShcD was altering EGFR subcellular localisation under basal conditions, we wanted to evaluate plasma membrane-associated EGFR for further evidence of differential partitioning. Accordingly, we performed surface labelling of non-permeabilized cells held at 4°C. The intensity of the resulting EGFR signal was demonstrably lower in ShcD-expressing cells when compared against their adjacent non-transfected counterparts (Fig. 2D). This discrepancy was captured by masking individual ShcD cells, measuring their mean red channel (EGFR) fluorescence, and expressing the values relative to those of non-transfected neighbours in the same fields of view. ShcD-positive cells were found to differ significantly in their surface EGFR reactivity, which was on average only 48% that of adjacent non-transfectants (Fig. 2E). However, ShcD was not found to reduce the total amount of EGFR in cells (Fig. 2F), thereby confirming that the adaptor alters EGFR subcellular localisation rather than overall expression. Taken together, these findings bolster the hypothesis that ShcD reduces surface presentation of the EGFR.

ShcD removes EGFR from the membrane, and associates with perinuclear endocytic recycling compartments

We next wanted to assess whether the internal receptor fraction was actively exchanged with the surface population, or whether it was sequestered upon synthesis and retained indefinitely in a distinct intracellular pool. Techniques similar to our surface labelling approach have been used previously under standard culture conditions to evaluate constitutive recycling of the EGFR (Rush and Ceresa, 2013). In this context, anti-EGFR antibody (clone 528) has been shown to bind and traffic with surface-exposed receptor without inciting activation (Dinneen and Ceresa, 2004). To verify that this was likewise the case in the COS-1 line, we exposed wild-type cells to antibody or ligand for 15 min, and immunoblotted for tyrosine phosphorylation (Fig. 3A). Receptor activation was only detected in the ligand-stimulated samples, suggesting that the antibody did not function as an agonist and could therefore be used to study basal-state receptor dynamics. Accordingly, we incubated live, ShcD- or GFP-expressing cells in an antibody preparation at 37°C for 2 h, fixing and analysing samples at six time points therein. A schematic representation (Fig. 3B) depicts canonical cellular

Journal of Cell Science (2017) 130, 2808-2820 doi:10.1242/jcs.198903

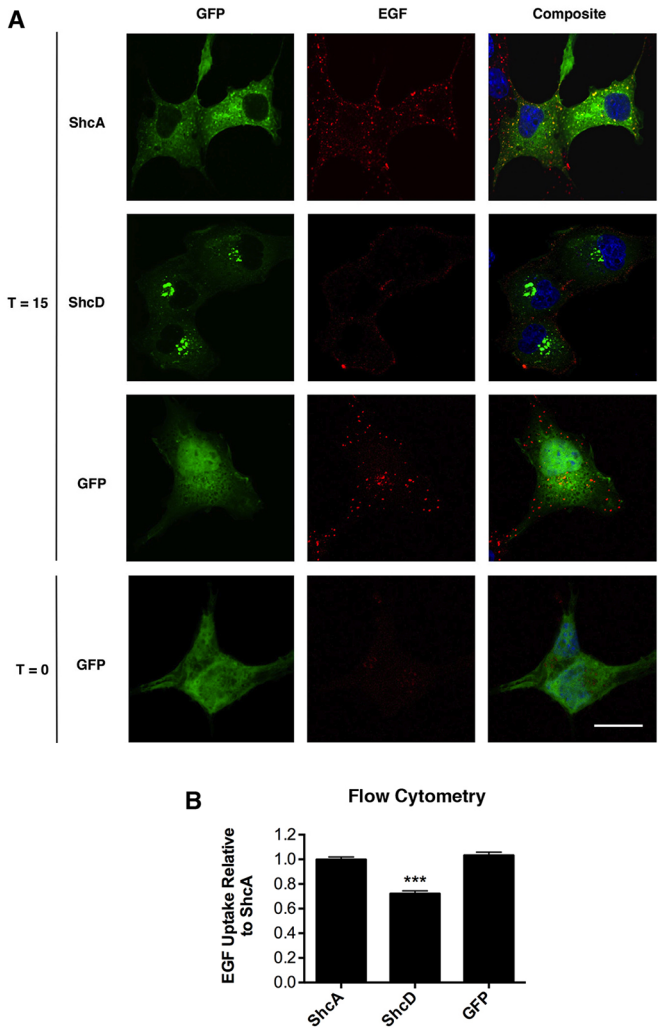

Fig. 1. ShcD expression reduces cellular acquisition of EGF. (A) Confocal microscopy was performed on fixed COS-1 cells expressing N-terminally GFP-tagged ShcA, ShcD or GFP alone, pulsed with EGF conjugated to Alexa Fluor 555 at 4°C followed by a 15 min chase (T=15) at 37°C. Control cells remained unstimulated (T=0). ShcD-induced reduction in EGF uptake was found across 13 independent biological replicates and numerous technical replicates therein. Scale bar: 20 µm. (B) Cells expressing the same ShcA, ShcD and GFP constructs as in A were analysed by flow cytometry to compare relative levels of acquisition of EGF conjugated to Alexa Fluor 647, which is depicted relative to ShcA. ShcD transfectants exhibited reduced ligand uptake compared to both ShcA and GFP (n=3, error bars denote s.e.m.). ***P=0.0001 (one-way ANOVA followed by Tukey's multiple comparison test).

acquisition of the fluorescent antibody raised against the N-terminus of EGFR. Fig. 3C shows representative ShcD-positive cells imaged 5 and 120 min after antibody administration. Robust, consistent overlap of ShcD with EGFR was evident by the end of the time course, as additionally captured by the cross-correlation function (CCF) arising from van Steensel colocalisation analysis (Fig. 3C; Table S1). Targeted recruitment of labelled EGFR to ShcD foci suggests that the receptor was indeed trafficking from the membrane. Mean red fluorescence values calculated as above from epifluorescence images (Fig. 3C, 'total signal') also revealed that the EGFR intensity ratio of ShcD-positive cells relative to adjacent non-transfectants (NTF) began to increase after 30 min. While the surface-labelled EGFR signal was initially weaker in the presence of ShcD, it eventually approached values consistent with those of wild-type cells (Fig. 3D). Notably, however, this signal boost was due to the formation of sharply demarcated ShcD-associated puncta, as opposed to the more uniform distribution of antibody over the cell surface, as was observed in control cells (Fig. 3C, T=120 min). Indeed, by comparison, the GFP:NTF ratio did not deviate significantly from 1, nor did it change substantially between 5 and 120 min. Overall, this suggests that ShcD recruits EGFR from the cell surface, and that these internalised receptor cohorts are continuously exchanging with the membrane population, albeit with different kinetics than those of control cells (Fig. 3G).

Having consistently observed ShcD and EGFR colocalising at juxtanuclear vesicles, we next endeavoured to identify the associated subcellular compartment. We evaluated three different markers, EEA1, CD63 and Rab11 (also known as Rab11a), which are affiliated with early, late and recycling endosomes, respectively. The top two rows of Fig. 3E depict the conventional scenario whereby ShcA distributes diffusely throughout the cytoplasm prior to stimulus, and frequently converges upon vesicles that are positive for EEA1 following ligand exposure. Since ShcD assumes a punctate appearance in the absence of EGF, we focused specifically on this unstimulated state for the purposes of vesicle identification. The pattern of EEA1 reactivity was found to be dense, ubiquitous and somewhat variable with respect to ShcD. Row 3 of Fig. 3E depicts a cell in which the overlap between the two proteins was negligible (Fig. 3E; Table S1). While ShcD appeared to associate intermittently with early endosomes, there was clearly no discernible relationship between the adaptor and CD63, which is enriched in multivesicular bodies (MVBs) and exosomes (Pols and Klumperman, 2009) (Fig. 3E, row 4).

In light of its nuclear proximity, we reasoned that ShcD might accumulate at Rab11-positive endocytic recycling compartments (ERCs) situated in this vicinity (Tomas et al., 2014). Indeed, co-expression of ShcD–GFP and Rab11–CFP produced evident regions of colocalisation, which were more consistent than those observed with EEA1 (Fig. 3E; Table S1). This trend was reflected in the mean correlation coefficients calculated across multiple replicates for each marker (Fig. 3F). Of the three vesicle types evaluated, Rab11-positive ERCs appeared to be the most positively correlated with ShcD. Although we did not undertake three-way analyses involving EGFR, our findings previously indicated that the receptor is tightly associated with ShcD puncta (Fig. 2), thereby suggesting that it is present in ERCs.

Considering these observations, we propose that ShcD promotes constitutive EGFR internalisation and accumulation in ERCs, thereby reducing the receptor population at the cell surface and decreasing the sensitivity of the cell to EGFR-mediated signals (Fig. 3G). Continuous exchange of the intracellular EGFR pool with the membrane allows for eventual acquisition of exogenous ligand or antibody, as demonstrated in our assay.

ShcD binds Cbl and promotes EGFR ubiquitylation

The ability of ShcD to induce aberrant endocytic patterns and premature vesicular inclusion indicates alterations to trafficking regulators, potentially including ubiquitin. Adhering to the prevailing belief that EGFR ubiquitylation is predominantly required for lysosomal targeting, and considering that the presence of ShcD does not decrease the total amount of EGFR protein, we predicted that the receptor would not be modified upon exposure to ShcD. Contrary to expectations, however, EGFR bound ubiquitin under serum-deprived conditions specifically when ShcD was present (Fig. 4A). This suggests that ShcD enhances ubiquitin

Journal of Cell Science (2017) 130, 2808-2820 doi:10.1242/jcs.198903

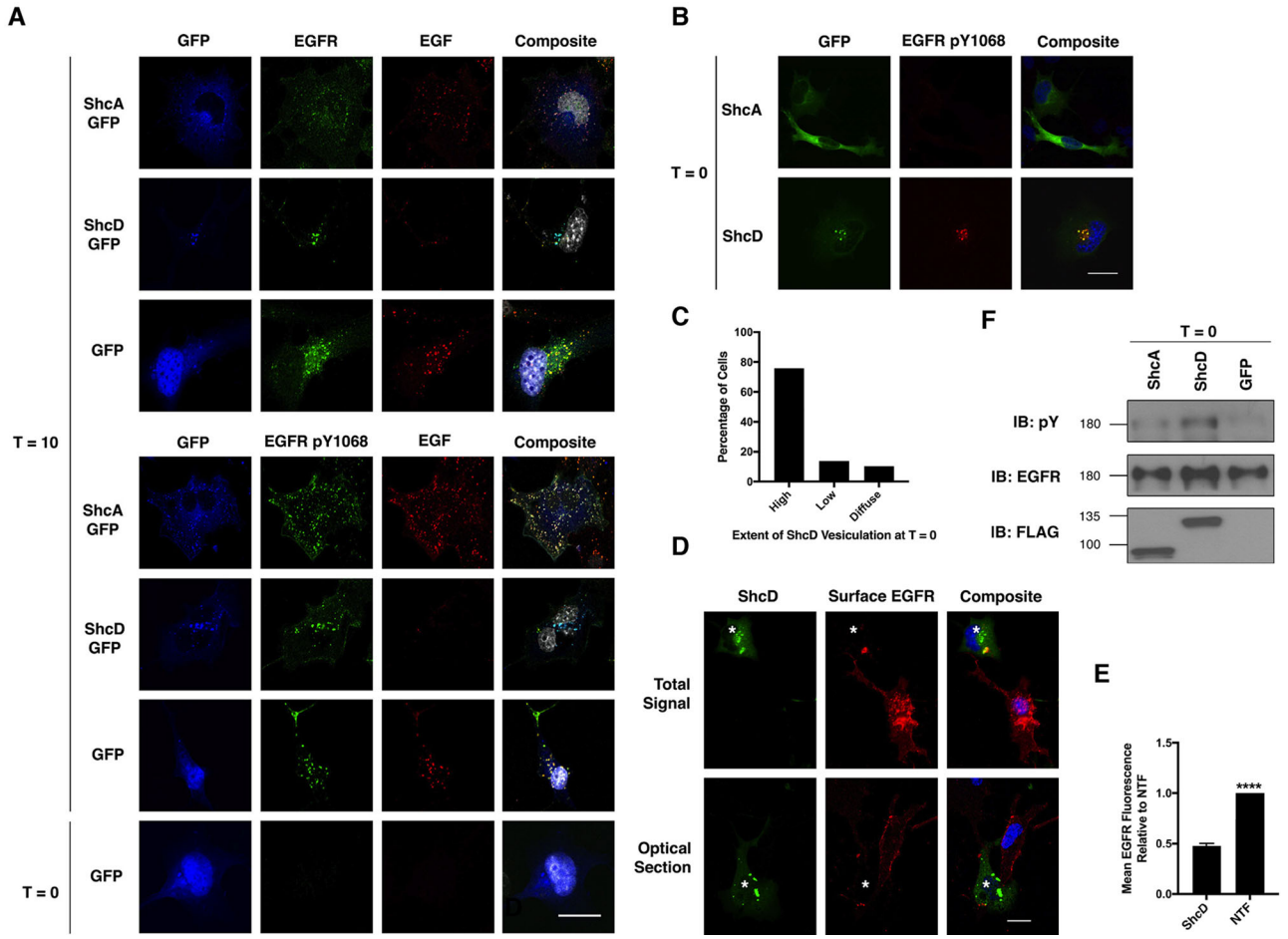

Fig. 2. EGFR is sequestered in the cell in the presence of ShcD. (A) Cells expressing ShcA–GFP, ShcD–GFP, and GFP alone were stained to detect the distribution of total EGFR and EGFR phosphorylated on residue Y1068 following a 10 min pulse (T=10) with 100 ng/ml EGF conjugated to Alexa Fluor 647, as compared to an untreated control (T=0). Artificially coloured four-channel detection allowed simultaneous assessment of the GFP-tagged species (blue), EGFR or pEGFR (green), EGF (red) and nucleus (grey). Distributions of ShcD with each of EGFR and pEGFR were independently confirmed following stimulation with untagged ligand (not shown). (B) The subcellular distribution patterns of ShcA and ShcD and the phosphorylation status of EGFR were evaluated under serum-deprived conditions. (C) We further classified the degree of ShcD vesiculation in 145 cells across 51 unique fields of view, placing cells in one of three categories ranging from high internal ShcD structure to diffuse appearance. (D) The extent of EGFR at the plasma membrane was compared between serum-starved ShcD-expressing cells and adjacent non-transfectants subjected to surface immunofluorescent labelling (60 min, 4°C). Output is shown as epifluorescent (total) signal and as a confocal optical section. White asterisks demarcate ShcD-expressing cells. (E) Mean red (EGFR) fluorescence in D was measured in individual adjacent transfected and non-transfected (NTF; control) cells in multiple fields of view across two biological replicates. ****$P<0.0001$ (*t*-test with Welch's correction). (F) Lysate from ShcA-, ShcD- and GFP-expressing cells was analysed by immunoblotting (IB) to detect tyrosine phosphorylation (pY) and levels of endogenous EGFR. Scale bars: 20 µm.

conjugation in the absence of exogenous signals that would typically initiate this event.

Indeed, whole-cell lysate probed for HA–Ub revealed a strong, multi-band smear corresponding only to ShcD-expressing samples (Fig. 4C, top panel). EGF stimulated GFP-positive cells were included for reference (Fig. 4C, top immunoblot, far right lane), and although the presumptive EGFR band was clearly visible, the ubiquitin signal was weaker, and consisted of fewer bands than that obtained under basal conditions with ShcD. Despite this evidence of elevated ubiquitin conjugation in the presence of ShcD, total levels of EGFR remained stable, suggesting that the modification did not accelerate protein degradation. Paradoxically, we also observed that the co-expression of HA–Ub with ShcD appeared to further enhance EGFR tyrosine phosphorylation above the normal threshold elicited by ShcD (Fig. 4A and C, compare lanes 1 and 2).

Traditionally, EGFR ubiquitylation occurs either by direct binding of the E3 ubiquitin ligase Cbl to the receptor (Grøvdal et al., 2004) or its indirect recruitment by Grb2 (Huang et al., 2006). As ShcD is a multivalent Grb2 adaptor, we questioned whether removing its recognition motifs would affect the ubiquitylation profile. ShcD Y6F is a tyrosine-to-phenylalanine mutant in which all six sites of inducible phosphorylation, including three Grb2 consensus sequences, have been rendered unmodifiable (Fig. 4B) (Jones et al., 2007; Wills et al., 2014). As shown in Fig. 4C, compound mutation of these sites did not alter the ubiquitin response elicited by ShcD, suggesting the involvement of an alternative mechanism that is independent of the CH1-region tyrosine phosphorylation status of ShcD.

Intriguingly, ubiquitylation also appears to proceed irrespective of direct Cbl–EGFR interaction, as our previous quantitative phosphoproteomic characterisation of the receptor indicated that the Cbl-binding site, Y1045, is not induced by ShcD (Wills et al., 2014). We additionally verified the lack of response by using an antibody specific to this phosphomotif (Fig. 4D).

Journal of Cell Science (2017) 130, 2808-2820 doi:10.1242/jcs.198903

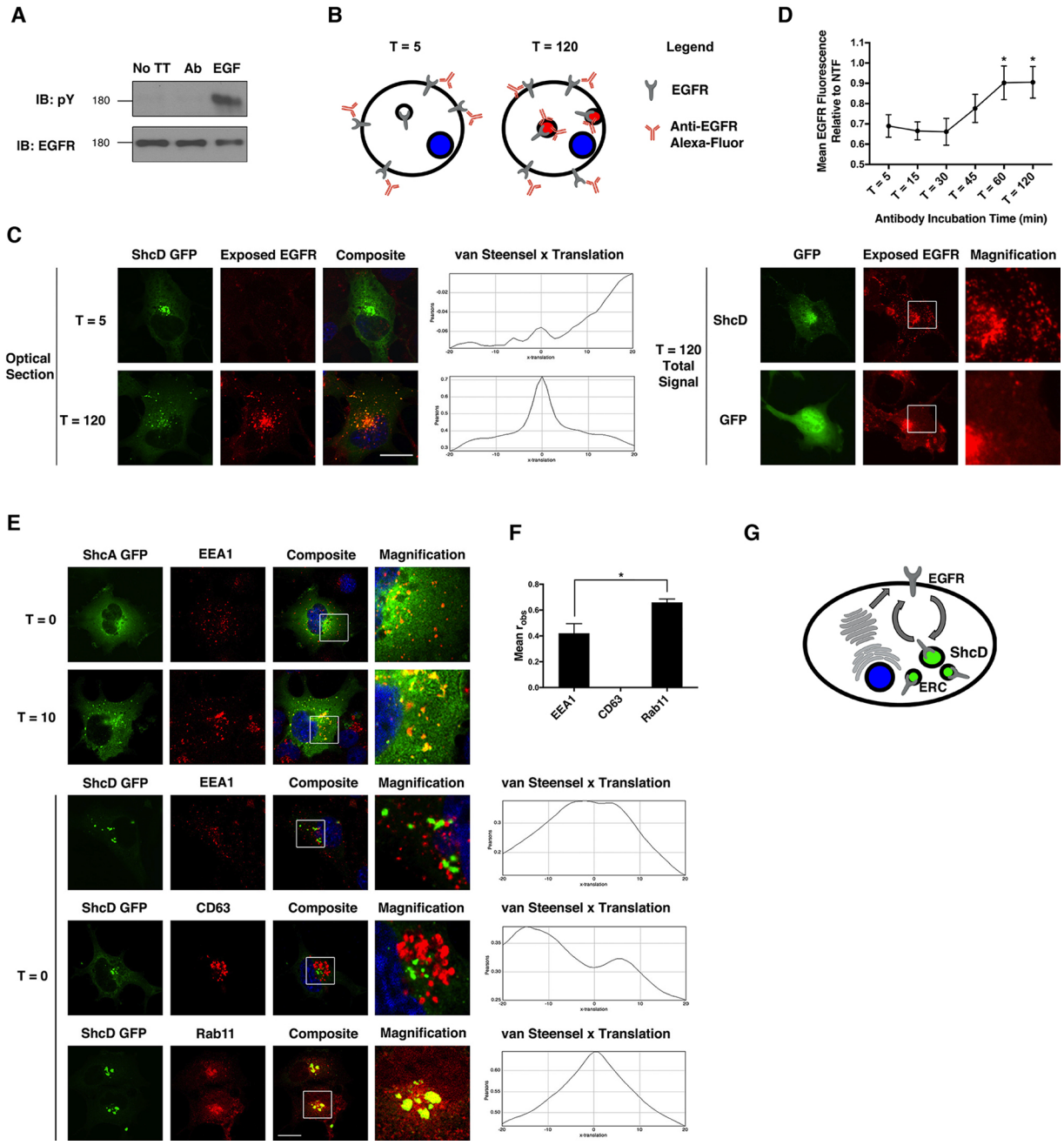

Fig. 3. ShcD removes EGFR from the cell surface, collects at Rab11-positive vesicles. (A) Wild-type COS-1 cells were incubated at 37°C for 15 min with anti-EGFR antibody (Ab), ligand (50 ng/ml; EGF) or left untreated (No TT) to compare the capacity of the supplements to induce EGFR phosphorylation. Lysate from these cells was analysed by immunoblotting (IB) to detect tyrosine phosphorylation (pY) and levels of endogenous EGFR. (B) Schematic rendering of the canonical response of live cells to exogenous anti-EGFR antibody. (C) Unstimulated ShcD-expressing cells were incubated with the same anti-EGFR antibody as in A, fixed, and assessed by confocal microscopy (Optical Section) at 5 min and 120 min to determine the extent of ShcD and EGFR colocalisation (van Steensel x Translation). Images were also acquired by standard epifluorescence microscopy (Total Signal) and used to measure mean red channel (EGFR) fluorescence in individually masked cells. An average of 16 pairs of cells from numerous fields of view across two biological replicates at six time points were measured to determine the mean grey value of the EGFR fluorescent signal. (D) Using values acquired in C, intensity of ShcD cells was expressed relative to non-transfectants in the same field of view (ShcD/NTF) and plotted. Following automated removal of outliers, the 5 min time point was compared to T=60 and T=120 via Kruskal–Wallis one-way ANOVA (P=0.0126) and Dunn's multiple comparison test (T5 vs T 60 min, P=0.0376; T5 vs T120 min, P=0.0197). (E) Recruitment of ShcA to early endosomes was assessed via the early endosomal antigen 1 (EEA1) marker applied to fixed cells subsequent to serum starvation (T=0) or an EGF pulse followed by a 10 min internalisation period (T=10). Subcellular localisation of ShcD–GFP in serum-deprived cells was determined by EEA1 and CD63 staining, and by co-transfection with Rab11–CFP. Magnified regions of interest are marked in the composite image. The extent of agreement between the Shc signal and each compartment marker was expressed as a Pearson's correlation coefficient, and further evaluated by van Steensel x-translation. (F) Averaged Pearson's r values (r_{obs}) representing the degree of colocalisation of ShcD with the three markers at T=0 across multiple cell and a minimum of two biological replicates are plotted. CD63, which failed in every replicate to meet criteria for significance (r_{obs}>r_{rand}, ≥95%), was assigned a value of 0 and omitted from subsequent analysis. *P=0.0105 between EEA1 and Rab11 (Welch's t-test). (G) Collectively, the data demonstrate that ShcD-expressing COS-1 cells differentially partition EGFR between the plasma membrane and Rab11-positive ERCs, thereby reducing cell surface presentation of the receptor. Internal and external EGFR populations are also found to be in continuous flux. Error bars denote s.e.m. Scale bars: 20 µm.

Journal of Cell Science (2017) 130, 2808-2820 doi:10.1242/jcs.198903

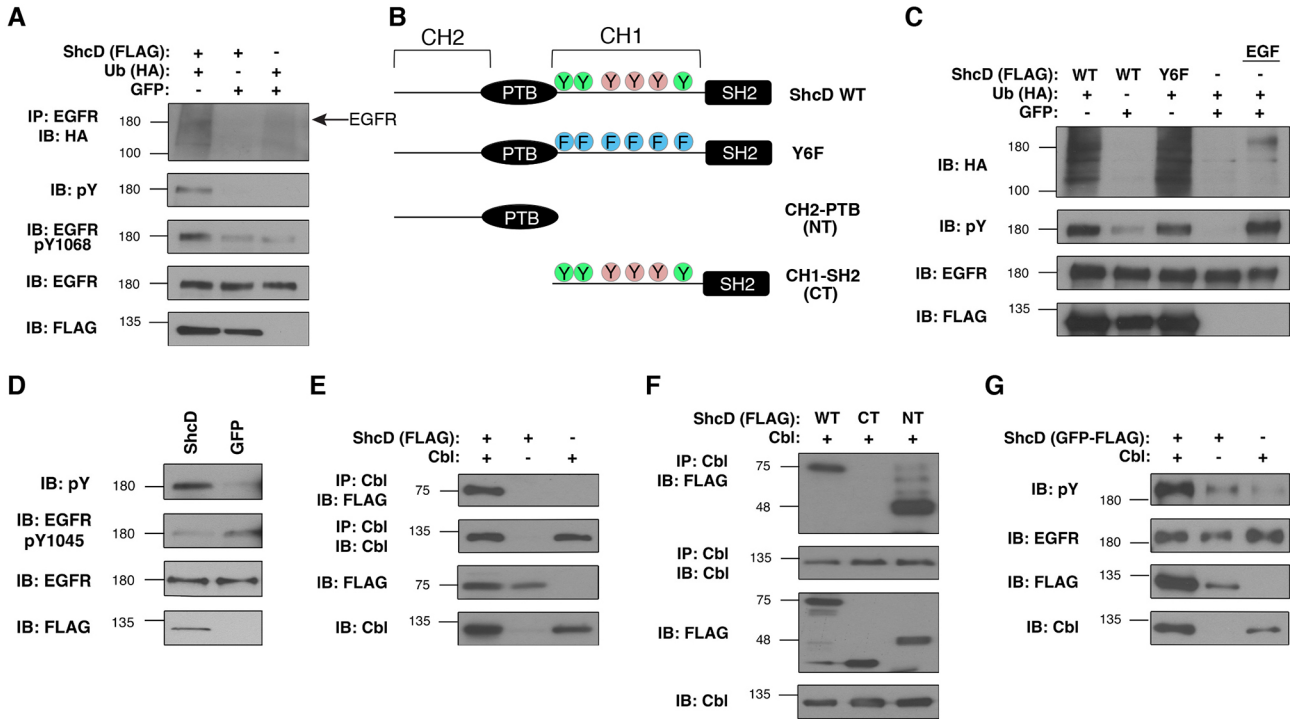

Fig. 4. ShcD binds Cbl and facilitates EGFR ubiquitylation. (A) Ubiquitylation of the unstimulated EGFR was assessed in the presence of overexpressed ShcD–GFP–FLAG and Ub–HA by immunoprecipitating (IP) EGFR and immunoblotting (IB) for the HA epitope. Immunoblots for tyrosine phosphorylation (pY), EGFR, and ShcD (FLAG) were performed in parallel to monitor total protein levels and assess the consequences of ubiquitin overexpression on receptor phosphorylation. (B) Schematic representations of the ShcD protein and laboratory-generated mutants. (C) Wild-type and mutant ShcD lacking CH1 region tyrosine residues (both GFP- and FLAG-tagged) were compared in their capacities to influence ubiquitin (Ub–HA) conjugation. (D) Unstimulated cells expressing either ShcD–GFP–FLAG or GFP alone were assessed using an antibody specific for the phosphorylated EGFR residue Y1045 in the Cbl-binding motif. (E) The potential of Cbl–HA and ShcD–FLAG to interact was pursued by expressing the proteins in HEK 293T cells, immunoprecipitating Cbl, and probing for ShcD (FLAG). (F) Likewise, the association was further characterised by subjecting the ShcD C-terminal (CT) and N-terminal (NT) fragments, depicted in B, to Cbl-mediated co-immunoprecipitations. (G) The consequence of the ShcD–Cbl association on EGFR phosphorylation was evaluated in COS-1 cells.

The implication that ShcD itself may recruit ubiquitin machinery was borne out in a proteomic screen of binding partners, which identified Cbl. To confirm this interaction, we introduced both ShcD and Cbl into HEK 293T cells, which contain negligible levels of EGFR, and performed co-immunoprecipitations. Under basal conditions, Cbl was clearly able to precipitate ShcD (Fig. 4E). Moreover, using N- (NT) and C-terminal (CT) ShcD truncations (Fig. 4B), we ascertained that the Cbl interaction occurred via the N-terminal fragment of the ShcD protein, which contains the CH2 region and PTB domain (Fig. 4F). Notably, these findings position Cbl as a unique and constitutive binding partner of ShcD, and suggest a mechanism by which EGFR ubiquitylation may be enhanced in the presence of this adaptor.

Returning to the COS-1 cell model, we questioned whether the additional boost in EGFR phosphorylation that we observed with ShcD and ubiquitin would be recapitulated with the co-expression of ShcD and Cbl. As shown in Fig. 4G, pEGFR was indeed enhanced in the presence of both species, above the level of ligand-free phosphoinduction achieved by ShcD alone. Moreover, we noted that expression of both Cbl (Fig. 4E,G) and ubiquitin (Fig. 4A,C) had a modest to pronounced effect on the level of ShcD detected, prompting speculation that its association with ubiquitin machinery stabilizes ShcD protein.

The PTB and SH2 domains of ShcD influence cellular EGF acquisition

Our findings thus far have revealed an unusual capacity of ShcD to alter both posttranslational modification patterns and trafficking behaviours of the EGFR, which prompted us to characterise the molecular componentry of the response. As our previous investigations into EGFR–ShcD dynamics revealed vital roles for the ShcD PTB domain in binding the receptor and facilitating its ligand-independent phosphorylation (Wills et al., 2014), we therefore speculated that the domain might likewise enable ShcD to subvert canonical EGF(R) localisation. We first verified that a targeted mutation of the ShcD PTB domain (PTB*; R315Q) was largely capable of preventing ligand-independent phosphorylation of the EGFR at Y1068 (Fig. 5A). Meanwhile, ShcD with the equivalent mutation in the SH2 domain (SH2*; R548K) retained the capacity to prematurely induce EGFR phosphorylation. The compound ablation of both domains (PTB*/SH2*) was found to behave in a similar fashion to the PTB* mutation alone, albeit with slightly more penetrance (Fig. 5A). Following stimulation, phosphorylated EGFR was identified in punctate structures where it failed to colocalise with the ShcD PTB*/SH2* mutant, thus suggesting that the receptor was relieved of ShcD control and was responding to exogenous EGF (Fig. 5A, bottom row).

To determine whether EGF internalisation was indeed restored in cells expressing a ShcD mutant that cannot bind EGFR, samples were pulsed at 4°C with EGF and assessed after a 15-min chase at 37°C (Fig. 5B). As anticipated, ShcD PTB*/SH2* transfectants demonstrated a consistent capacity to amass ligand, albeit in vesicles that were distinct from those of the ShcD compound mutant (Fig. 5B, second row). Clearly, abolishing the tyrosine binding function of both domains conferred the most complete

Journal of Cell Science (2017) 130, 2808-2820 doi:10.1242/jcs.198903

protection from ShcD-induced EGFR hyperphosphorylation and sequestration.

The AP2 motif affects Shc subcellular localisation and facilitates adaptin binding

A distinguishing feature of ShcD is the absence of the CME-associated AP2-binding region that is otherwise conserved across the Shc adaptor family. This evolutionary loss was therefore a prime candidate in our search for molecular determinants of ShcD-mediated trafficking defects. However, the AP2 consensus sequence is among the least studied attributes of the Shc proteins, so our strategy to address its contributions involved mutagenic characterisation of both ShcA and ShcD. Under the hypothesis that differential recruitment of AP2 adaptins, clathrin, and endocytic machinery might establish distinct fates for ShcA versus ShcD, we removed the AP2 motif (AD) from wild-type ShcA, and inserted the sequence into the equivalent location of the wild-type ShcD backbone. The resulting proteins are henceforth designated ShcA-ΔAD and ShcD-AD, respectively (Fig. 6A). Previously, the utility of the AD motif was evaluated in the context of ShcA via two targeted phenylalanine-to-alanine mutations that are known to disrupt adaptin binding (Sakaguchi et al., 2001). We likewise recapitulated this particular mutation in ShcD-AD, to generate ShcD-FA (Fig. 6A).

We first confirmed that this motif in ShcA facilitates receptor internalisation. The upper two rows of Fig. 6B depict the canonical ligand response of ShcA, characterised by recruitment of the adaptor to EGF- and pEGFR-positive vesicles. By contrast, only minor vesiculation of ShcA-ΔAD was evident at the 10-min time point, and this corresponded to reduced EGFR activation, and minimal EGF uptake (Fig. 6B). Notably, ShcA-ΔAD was enriched in the nucleus both before and after stimulation (Fig. 6B). This unexpected nuclear accumulation prompted us to search the excised region for a localisation signal that could explain the atypical distribution. *In silico* analysis (la Cour et al., 2004) revealed that the sequence MKPFEDALRV, which overlaps extensively with the consensus AP2-binding motif, possesses characteristics of a nuclear export signal (NES) (Fig. S1, Table S2).

Taking the complementary approach using chimeric ShcD containing the transplanted AP2 region, we initially verified that the isolated peptide corresponding to this stretch of the CH1 region was able to bind to α-adaptin in cellular lysates, and that this interaction was disrupted in the FA mutation (Fig. 6C). Lysates recovered from cells expressing the chimeric proteins were subject to co-immunoprecipitation experiments to evaluate the adaptin-binding potential of modified ShcD. As shown in Fig. 6D, the addition of the AD motif substantially enhanced the ShcD–adaptin interaction. FA mutations within the sequence reduced co-precipitation of FLAG-tagged ShcD with α-adaptin, but did not diminish the interaction to the level of wild-type ShcD (Fig. 6D).

Confocal microscopy yielded consistent findings at the level of individual cells. The absence of adaptin colocalisation noted in ShcD wild-type cells was rectified with ShcD-AD, and largely lost in cells expressing ShcD-FA (Fig. 6E).

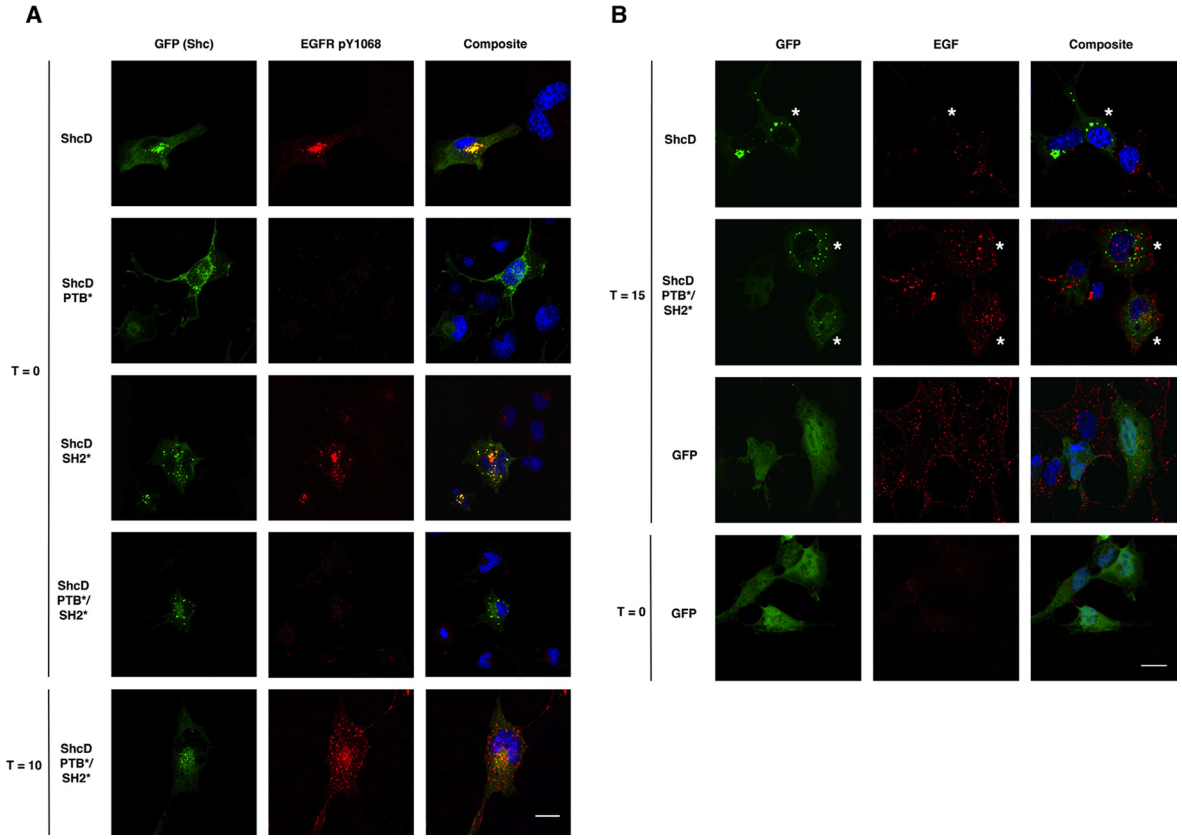

Fig. 5. The ShcD tyrosine-binding domains enable EGFR hyperphosphorylation and sequestration. (A) Single amino acid mutations in the ShcD PTB domain (PTB* R315Q) and/or SH2 domain (SH2*; R548K) that disrupt phosphotyrosine-mediated interactions (Wills et al., 2014) were used to evaluate the contributions of the domains on EGFR phosphorylation status and localisation. Confocal microscopy images depict both the transfected cell of interest (green) and surrounding non-transfectants for reference. (B) Similarly, the ShcD PTB*/SH2* mutant was compared against the wild-type protein and GFP to evaluate its influence over ligand uptake. ShcD-expressing cells are denoted with white asterisks. Scale bars: 20 µm.

Journal of Cell Science (2017) 130, 2808-2820 doi:10.1242/jcs.198903

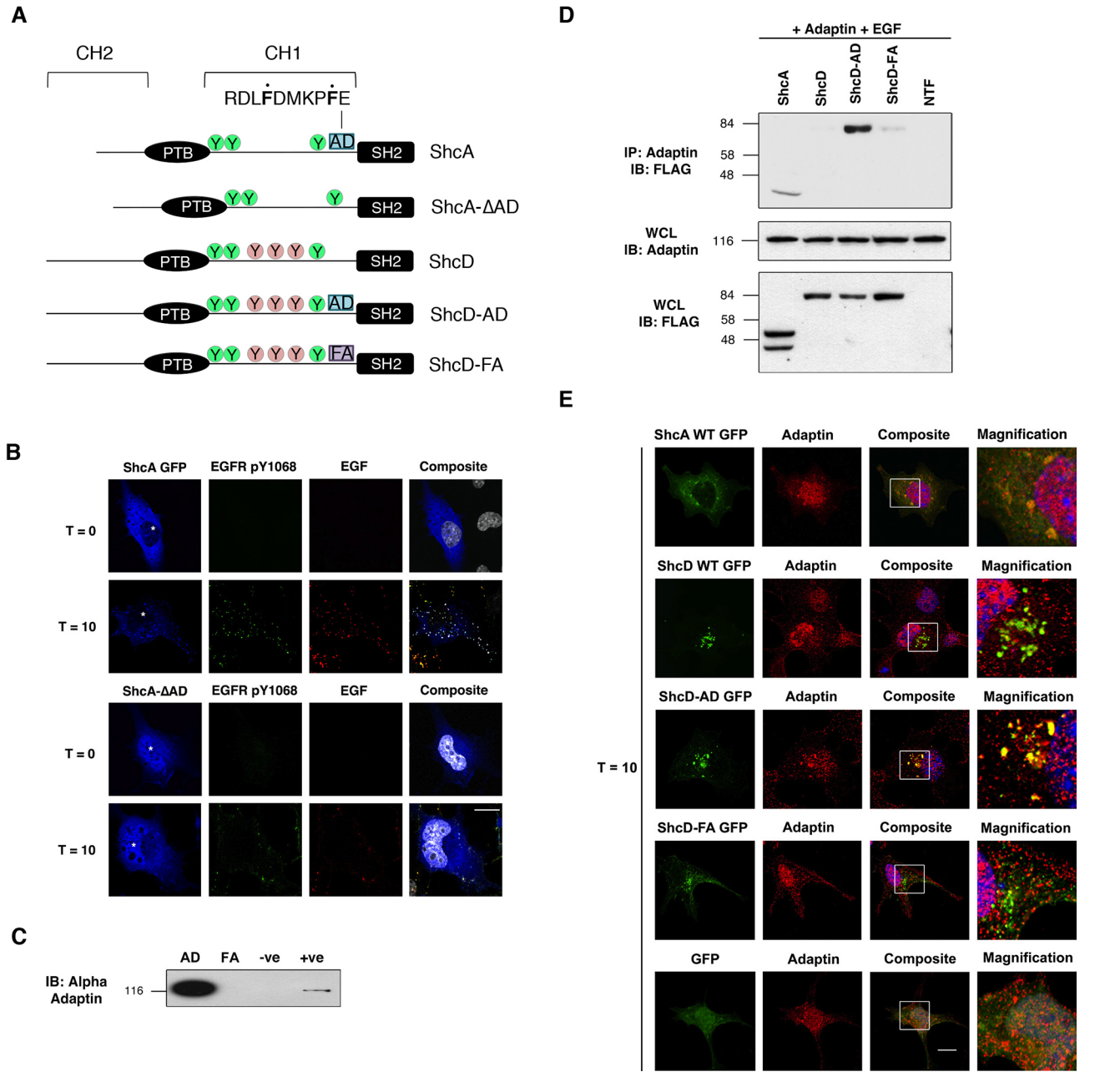

Fig. 6. The ShcA AP2 recognition motif influences subcellular localisation, and enables adaptin binding when introduced to ShcD. (A) Schematic comparison of ShcA and ShcD proteins, depicting the conserved adaptin-binding motif (AD) identified by Sakaguchi et al. (2001), which is absent from ShcD, and was experimentally removed from ShcA to generate ShcA-ΔAD. The wild-type AP2 region and disabling Phe to Ala (FA) mutant (mutated residues denoted in bold with a dot above) were also introduced into the analogous region of ShcD to generate chimeric adaptors. (B) ShcA-ΔAD cellular distribution and influence on EGFR phosphorylation and ligand acquisition (100 ng/ml EGF conjugated to Alexa Fluor 555) were compared against that of the wild-type protein. White asterisks demarcate nuclei. (C) Peptides corresponding to the AD and FA motifs were assessed by immunoblotting (IB) to confirm their adaptin-binding capacity. –ve, beads alone; +ve, immunoprecipitation (IP) of α-adaptin. (D) Chimeric ShcD–FLAG constructs depicted in Fig. 5A were expressed in cells, and resulting lysates were subjected to co-immunoprecipitation to determine whether the transplanted sequence endowed ShcD with adaptin-binding functionality. NTF, no Shc transfected; WCL, whole-cell lysate. (E) The subcellular localisation of Shc–GFP–FLAG relative to α-adaptin was evaluated in cells expressing the wild-type, Shc-AD and ShcD-FA chimera variants, following a 10 min EGF stimulation (T=10). Magnified regions of interest are shown boxed in the composite image. Scale bar: 20 µm.

Chimeric ShcD containing the AP2 motif promotes EGF internalisation

Beyond the initial characterisation of binding potential, it remained to be seen whether ShcD-AD would preserve the unique attributes of wild-type ShcD, and/or acquire sufficient ShcA functionality to mimic the cellular dynamics of the canonical adaptor. To investigate the effect of this chimera on EGFR dynamics, we first evaluated whether ShcD-AD retained the capacity to elicit EGFR hyperphosphorylation, which is a hallmark of wild-type ShcD. Fig. 7A demonstrates that ShcD-AD could indeed be identified in punctate form, colocalised with EGFR pY1068 both before and after stimulus. However, while expression of wild-type ShcD largely excluded ligand, ShcD-AD permitted EGF internalisation, and was found to localise with the resulting puncta (Fig. 7B). Much

Journal of Cell Science (2017) 130, 2808-2820 doi:10.1242/jcs.198903

of this uptake and association were lost with ShcD-FA. Flow cytometry confirmed that EGF acquisition was significantly enhanced in cells expressing ShcD-AD, as compared to those transfected with the wild-type protein (Fig. 7C). ShcD-FA was also found to increase ligand uptake, though not to the same extent as the unmodified AD motif, consistent with reduced adaptin binding demonstrated in Fig. 6D. This striking result demonstrates that the gain of AP2-binding functionality in ShcD does indeed influence the EGF(R) equilibrium in the cell. In its wild-type form, ShcD appears less capable of participating in canonical EGFR trafficking.

The change in EGF internalisation dynamics elicited by ShcD-AD also suggests a corresponding alteration in EGFR trafficking behaviour. To determine whether the transplanted AP2 motif had any bearing on the subcellular compartment associated with ShcD, we evaluated EEA1 reactivity, and identified regions of overlap with ShcD-AD both before and after ligand stimulus, when the adaptor was found in punctate structures (Fig. 7D; Table S1). Overall, ShcD-AD demonstrated a slight but statistically significant increase in post-stimulus EEA1 colocalisation relative to wild-type ShcD (Fig. 7E).

Similarly, we compared steady-state, membrane-associated EGFR populations using surface labelling and single cell fluorescence measurements, in addition to categorical cellular phenotyping. In so doing, we discovered that while EGFR labelling was predictably low in cells expressing wild-type ShcD, EGFR reactivity was notably upregulated in the presence of ShcD-AD, and took on a predominantly punctate appearance (Fig. 7F). The mean red fluorescence values differed significantly between the two treatments (Fig. 7G), thereby suggesting that ShcD-AD cells sustain a larger fraction of EGF receptors at the cell surface.

Considering its contributions as a NES, a binding motif for CME componentry, and a regulator of EGFR membrane partitioning, the AD region endows its native proteins with multiple functionalities that appear to be absent in wildtype ShcD.

ShcD alters EGFR phosphorylation and localisation in a model of glioma

Our previous discovery that ShcD is upregulated in a variety of human gliomas (Wills et al., 2014) prompted us to determine whether ShcD-induced EGFR phosphorylation and trafficking perturbations could be recapitulated in relevant *in vitro* models. A431 human epidermoid carcinoma cells and N19 murine oligodendrocytes both failed to elicit ShcD-mediated EGFR phenomena under our assessment protocols (data not shown). In U87 glioblastoma cells, preliminary work revealed that pEGFR was undetectable following stimulation (data not shown), so EGFR was introduced to this line via transfection. Cells are depicted in Fig. 8 in the serum-deprived state. In singly-transfected cells, ShcD was found to be diffuse, and pEGFR was negligible. However, when the proteins were co-expressed, EGFR was phosphorylated at residue Y1068, and found to colocalise with ShcD near the nucleus. Surprisingly, co-transfection of EGFR and ShcD also elicited a considerable morphological change characterised by a loss of polar extensions and an increase in cell body size, compared to the slender bipolar morphology adopted by single and non-transfectants. These findings demonstrate that although the ShcD-induced phenotype is not universal, there are physiologically applicable circumstances under which it is provoked.

DISCUSSION

The impetus to study the contributions of ShcD to EGFR trafficking arose from our earlier discovery that the adaptor alters the phosphotyrosine profile of the receptor (Wills et al., 2014), and also lacks the endocytosis-associated AP2 motif that is otherwise conserved across the Shc family (Fagiani et al., 2007; Jones et al., 2007). We now demonstrate that expression of ShcD differentially partitions EGFR between the plasma membrane and Rab11-positive ERCs, where it is prematurely phosphorylated, ubiquitylated and sequestered from ligand. Accordingly, we show that Cbl is a novel ShcD-binding partner that likely accounts for the observed receptor hyperubiquitylation. Ligand-independent EGFR sequestration and phosphorylation are both circumvented in cells expressing loss-of-function phosphotyrosine-binding-defective ShcD, while the gain-of-function addition of the ShcA AP2-binding motif to the ShcD CH1 region restores receptor/ligand trafficking. The emerging picture thus positions ShcD not as a passive scaffold recruited to a stimulated receptor, but as an active signalling regulator that influences EGFR in various cellular networks. Indeed, the non-canonical nature of ShcD has been reinforced by our recent discovery that the adaptor suppresses ERK1/2 phosphorylation distal to neurotrophic receptors (Wills et al., 2017). Although signalling output was not examined in the present work, it is tempting to speculate that the EGFR mislocalization we describe herein could similarly disconnect the receptor from canonical pathways.

ShcD appears to be unique in its capacity to subvert classical EGFR trafficking, and although Shc and Cbl have previously been identified in signalling complexes following EGF stimulation, their association was believed to be mediated by Grb2 (Fukazawa et al., 1996). This is the first report of a constitutive interaction between a Shc protein and Cbl, and the only account of a Shc family member driving receptor ubiquitylation and subcellular partitioning. The fact that these proceed in the absence of exogenous signal is all the more intriguing and unusual.

Nevertheless, ubiquitin is increasingly regarded as a mechanistic component of EGFR endocytosis, beyond its role in lysosomal targeting (Fortian et al., 2015). Accordingly, the CME adaptor protein Epsin 1 associates with the receptor through ubiquitin-interacting motifs (UIM), and is a critical driver of EGFR internalisation, as is its partner, Eps15 (Carbone et al., 1997; Kazazic et al., 2009). Recently, the novel isoform Eps15S was found to regulate Rab11 ERC structure, function and EGFR recruitment (Chi et al., 2011), thus prompting us to speculate that ShcD-induced EGFR ubiquitylation may in fact enable receptor endocytosis and ERC accumulation.

In our search for trafficking-related sequences, the ShcA-ΔAD deletion mutant offers the first glimpse of the repercussions of complete AP2 motif removal. Importantly, it also mimics the evolutionary loss of AP2 that naturally occurred in ShcD. While we report that ShcA-ΔAD-expressing cells are less responsive to EGF stimulus, the ShcA mutant does not recapitulate ShcD-induced EGFR phosphorylation or subcellular localisation patterns, thus reinforcing that the proteins are unique and non-redundant. Indeed, the most striking feature of ShcA-ΔAD is its nuclear accumulation, which can be explained by a previously undocumented nuclear export sequence (NES) that coincides with the AP2 binding region. The signalling isoforms of ShcA are predominantly regarded as cytosolic adaptors (Wills and Jones, 2012), although p46 has been detected in the nucleus of select carcinomas (Yoshida et al., 2004; Yukimasa et al., 2005), while p52 interacts with nuclear import factors, and has been identified as a putative binding partner of nuclear proteins (George et al., 2009). Nevertheless, there appear to be no existing reports of NES sequences in the protein, and the nuclear utility of ShcA remains unknown. Although wild-type ShcD naturally lacks the AP2 motif, it seems to avoid constitutive

Journal of Cell Science (2017) 130, 2808-2820 doi:10.1242/jcs.198903

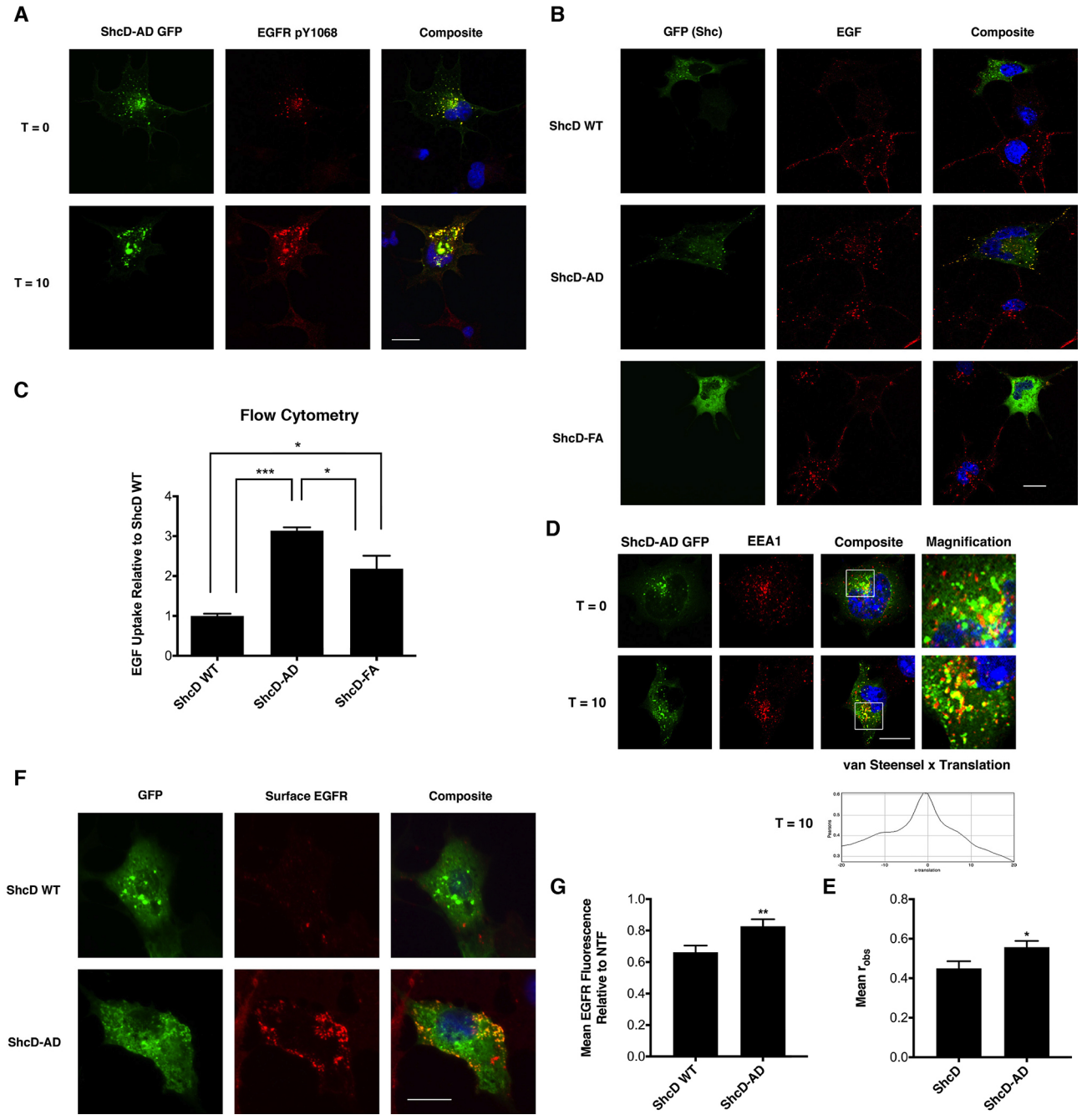

Fig. 7. An ectopic adaptin-binding motif in ShcD restores ligand internalisation. (A) Cells expressing ShcD-AD were stained with anti-EGFR pY1068 prior to (T=0) and following (T=10) EGF internalisation, to assess the influence of the chimeric region on EGFR hyperphosphorylation. (B) The effect of ShcD chimeric protein expression on EGF acquisition and distribution were assessed by confocal microscopy following administration of EGF conjugated to Alexa Fluor 555. (C) Flow cytometry revealed a statistically significant increase in the amount of EGF acquired by cells expressing ShcD-AD (n=3). (ANOVA P=0.0008; multiplicity adjusted P values of Tukey's comparison test: ShcD WT versus AD, ***P<0.001, ShcD WT and ShcD-AD vs ShcD-FA, *P<0.05.) (D) Confocal microscopy-based analysis of ShcD-AD colocalisation with EEA1, expressed as van Steensel x translation. (E) The resulting Pearson's r values (r_{obs}) representing the extent of overlap of EEA1 with each of ShcD and ShcD-AD following ligand stimulation (50 ng/ml, T=10 min) were averaged across at least 10 cells representing a minimum of two biological replicates. A Mann–Whitney test was performed to compare means (*P=0.0405). (F) Surface EGFR labelling of unstimulated cells was conducted at 4°C for 30 min, followed by epifluorescence microscopy, to assess EGFR surface distribution in cells expressing either wild-type ShcD or ShcD-AD. (G) Images captured from three biological replicates for experiments shown in F were used as a basis to measure mean red (EGFR) fluorescence across the two conditions, which were compared by Mann–Whitney test (**P=0.0017). Error bars denote s.e.m. Scale bars: 20 µm.

nuclear entrapment due to a separate NES identified in the CH2 region (Ahmed and Prigent, 2014).

Outcomes from our complementary gain-of-function ShcD-AD approach demonstrate that the chimera retains the potential to facilitate stimulus-independent EGFR phosphorylation, although it also permits internalisation of the receptor–ligand complex, and relocates to the resulting vesicles. By comparison, the PTB*/SH2* double mutant fails to colocalise with the receptor, and restores ligand acquisition due to its mutationally induced loss of influence over the EGFR. Thus, the rescues afforded by the two opposing

Journal of Cell Science (2017) 130, 2808-2820 doi:10.1242/jcs.198903

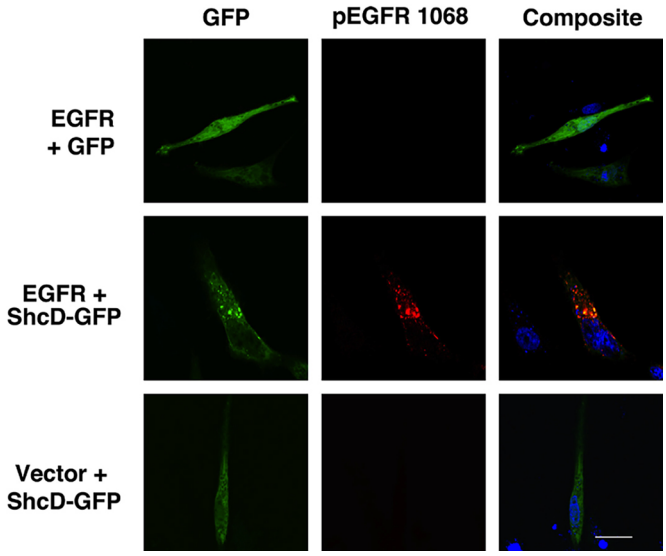

Fig. 8. ShcD alters EGFR distribution and cellular morphology in U87 glioma cells. U87 cells transfected with EGFR, ShcD or both, were analysed in serum-deprived conditions for EGFR pY1068. Scale bars: 20 µm.

strategies are fundamentally different. ShcD-AD uniquely appears to provoke a hybrid phenotype, displaying characteristics of both ShcA (EGF acquisition) and ShcD (EGFR hyperphosphorylation), which underscores that basal-state phosphorylation and vesiculation are not mutually exclusive to ligand responsiveness. These findings suggest that ShcD-mediated control of EGFR surface presentation and receptor phosphorylation are at least somewhat distinct, with the former manifesting as a loss of conserved function, while the latter represents a gain of novel function never before encountered in a Shc protein.

It is yet unclear how a consensus sequence for clathrin endocytosis machinery can have such a dramatic impact on cellular dynamics, considering the multiple redundancies that exist in receptor internalisation processes. Breaking direct EGFR contact with the adaptin complex only minimally affects EGFR internalisation (Nesterov et al., 1999; Sorkin et al., 1996), and accordingly, the prevailing evidence portrays the ShcA AP2 motif as a subtle modulator of EGFR CME as opposed to being a driving force (Sakaguchi et al., 2001). However, our findings suggest that transplanting the AD region increases EGF acquisition, post-stimulus EEA1 vesicle association, and the steady-state availability of receptor at the membrane. We therefore propose that instead of simply augmenting CME of a developing signalling complex, the AP2 sequence may help to connect ShcD, and any associated EGFR, with plasma membrane componentry. This could alter trafficking patterns and encourage EGFR–ShcD cycling between the cell cortex and cytoplasm by promoting increased ShcD membrane localisation, and mobilisation of sequestered vesicles. ShcD is notably lacking elements of a pleckstrin homology (PH) domain that are conserved across the rest of the family to target Shc to membrane phospholipids (Fagiani et al., 2007; Ravichandran et al., 1997). Moreover, AP2 adaptins are uniquely involved in endocytosis from the plasma membrane, and are not utilised in intracellular vesicle formation (McMahon and Boucrot, 2011), thus highlighting a potential role for membrane recruitment in the rescue.

Going forward, it will be of particular interest to determine why ShcD deviates so profoundly from the canonical Shc adaptor paradigm, and what greater physiological purpose is served by promoting constitutive EGFR phosphorylation, non-degradative ubiquitylation and accumulation in Rab11-positive compartments, rendering the cell less sensitive to ligand. Intriguingly, there are other circumstances that reproduce aspects of this phenotype. For example, the EGFR phosphorylation pattern that we observe with ShcD (activation of Y1068, Y1148 and Y1173, and suppression of Y1045) has also been documented in response to oxidative stress and oncogenic mutation, both of which are associated with atypical trafficking and defective downregulation of the receptor (Han et al., 2006; Ravid, 2002).

Indeed, EGFR internalisation strategies and destinations are heavily influenced by the instigating stimulus, and ShcD is not unique in directing EGFR to the vicinity of the nucleus. Oxidative stress exposure has been found to promote perinuclear retention of EGFR in a Src- and caveolin-1-dependent fashion (Khan et al., 2006). Similarly, EGF receptors containing the oncogenic activating mutations identified in non-small cell lung cancer (NSCLC) were observed to endocytose constitutively and recycle through Rab11-positive compartments, while ligand-activated wild-type EGFR was not detected in juxtanuclear structures (Chung et al., 2009). In both cases, aberrant EGFR activation and trafficking were associated with altered signalling potential.

This precedent is particularly relevant to our discovery that ShcD is upregulated in human gliomas, coinciding with enhanced EGFR phosphorylation (Wills et al., 2014). Although the ShcD–EGFR phenotype is not a universal phenomenon, altered EGFR activation and subcellular distribution are apparent in U87 glioma cells, which also undergo morphological changes as a result. To date, ShcD-mediated EGFR phosphorylation has been demonstrated in COS-1, HEK293 (Wills et al., 2014), CHO (M.K.B.W., unpublished observations) and U87 cells. Although the significance of EGFR–ShcD collusion to the mechanism of cancer progression remains to be seen, this work provides further evidence of a truly divergent role for the ShcD protein in growth factor signalling and trafficking dynamics.

MATERIALS AND METHODS

Plasmids, antibodies and cell supplements

Wild-type and domain-mutated forms of human ShcD were previously cloned into the pcDNA3 vector (Invitrogen) with a triple C-terminal FLAG epitope, and the pEGFP C2 vector (Clontech) to generate N-terminal GFP and C-terminal FLAG double tagging (Jones et al., 2007; Wills et al., 2014). The ShcA-ΔAD mutant was created by deletion mutagenesis PCR to excise the region corresponding to the protein sequence RDLFDMKPFEDALR. To construct ShcD containing a wild-type or mutated ShcA AP2 recognition site, the nucleotide sequence encoding 17 amino acids spanning the motif (SAPRDLFDMKPFEDALR) or FA mutation (SAPRDL**A**DMKPA**A**EDALR) was used to replace the analogous region in ShcD. CFP–Rab11 and HA–Ub were kindly provided by Jane McGlade (University of Toronto, Toronto, Canada) (Smith and McGlade, 2014).

EGF was utilized in its unlabelled form (PeproTech), or conjugated to Alexa Fluor 555 or 647 (Invitrogen) at concentrations of 50 to 100 ng/ml.

Primary antibodies were employed for immunoprecipitation (IP), immunoblotting (IB), and immunofluorescence (IF) to detect total protein, or phosphorylated moieties. Anti-α-adaptin, BD Transduction Laboratories, #610502, Lot# A43920 (IB: 1:1000); anti-c-Cbl, Santa Cruz Biotechnology, C-15, sc-170, Lot #D0214, (IF: 1:200); anti-CD63, Developmental Studies Hybridoma Bank, H5C6 antibody ID AB_528158 (IF: 1:50); anti-EEA1, BD Transduction Laboratories, #610456, Lot# 78952 (IF: 1:50); anti-EGFR, Santa Cruz Biotechnology, sc-03, Lot# B2610 (IB: 1:500, IF: 1:100); anti-EGFR conjugated to Alexa Fluor 647, Santa Cruz Biotechnology, clone 528, sc-120 AF647, Lot# H0415 (surface labelling IF: 1:200); anti-EGFR pY1068, Cell Signaling Technology, D7A5, Lot# 2 (IB: 1:1000, IF: 1:400); anti-FLAG, Sigma, M2, Lot# SLBJ4607V (F1804) (IB: 1:1000); anti-HA, 12CA5, provided by Daniel J. Dumont, University of Toronto (IB: 1:1000); and anti-pTyr, 4G10, Daniel J. Dumont (IB: 1:1000) antibodies were

used. Horseradish peroxidase (HRP)-conjugated goat anti-mouse-IgG and goat anti-rabbit-IgG secondary antibodies (Biorad) were used for immunoblot detection, while goat anti-mouse-IgG or goat anti-rabbit-IgG conjugated to Alexa Fluor 594 (Invitrogen) were employed for immunostaining.

Cell culture, transfection and stimulation

U87 cells were kindly provided by Dr Jane McGlade (University of Toronto) while HEK 293T and COS-1 cells were the generous gift of Dr Tony Pawson (University of Toronto). All lines were confirmed to be free of mycoplasma contamination, and were handled as previously described (Wills et al., 2014). Briefly, cells were maintained at 37°C, 5% CO_2 in Dulbecco's modified Eagle's medium (DMEM) supplemented with 10% fetal bovine serum (FBS) and 1% penicillin-streptomycin. Polyethyleneimine (PEI)-based plasmid transfection was performed 24 h after cell passaging, and expression allowed to proceed for a minimum of 24 h before cells were treated or processed. At 18 to 20 h prior to EGF stimulation, medium was removed from cells and replaced with serum-free DMEM containing 1% penicillin-streptomycin. EGF was applied to plates or wells at a final concentration of 50 ng/ml (untagged ligand) to 100 ng/ml (Alexa Fluor conjugates, enabling better visibility). Samples intended for microscopy or flow cytometry were incubated with EGF at 4°C for 30 min to facilitate ligand loading, rinsed with 1× phosphate-buffered saline (PBS), and warmed to 37°C in fresh DMEM to permit receptor internalisation for the indicated chase period.

Cell lysis, immunoprecipitation, peptide binding, immunoblotting

Cells were handled and harvested as described previously (Wills et al., 2014). To immunoprecipitate (IP) select proteins, fractions of total lysate were rotated overnight at 4°C in a mixture of primary antibody, 10% anti-mouse bead-conjugated secondary antibody, and PLC+ buffer. IPs were centrifuged for 1–2 min at 3000 rpm, washed with PLC buffer, and boiled briefly at 100°C in 2× SDS protein sample buffer to elute proteins.

Peptide binding was performed by incubating 5 µg of biotinylated peptide with cleared cell lysates for 2 h at 4°C, then processed and analysed as for immunoprecipitation. Peptides were generated on an AbiMed 431 synthesizer using standard Fastmoc techniques, with an N-terminal biotin group to facilitate recovery on streptavidin-conjugated agarose beads (Pierce). Products were confirmed by mass spectrometric and amino acid analysis. IP and whole-cell lysate samples combined with 2× SDS sample buffer were immunoblotted as described previously (Wills et al., 2014).

Flow cytometry

Cells destined for analysis were seeded in 35 mm wells, pulsed with 100 ng/ml EGF conjugated to Alexa Fluor 647 and warmed as described. Wells were then rinsed with 1× PBS to remove unbound ligand, and trypsinized in a small volume to suspend cells, which were then diluted to a final concentration of 1×10^6–2×10^6 cells/ml in DMEM containing FBS. A Beckman Coulter FC500 flow cytometer and MXP software were used for the analysis. Fluorescence was measured using FL-1 (488 nm) and FL-4 (647 nm) bandpass filters, and threshold was determined empirically by ensuring that fewer than 10% of non-transfected unstimulated control cells exceeded this value. Ligand uptake was calculated as {# green and red cells (i.e. yellow)}/{total # green cells}×100. The Brown–Forsythe test of equal population variance, one-way ANOVA and Tukey's multiple comparisons tests were performed in Graph Pad Prism 6.

Immunofluorescent staining, microscopy and image analysis

Surface labelling was performed using an Alexa Fluor 647-conjugated antibody raised against the N-terminal region of the EGFR (clone 528), at 1:200 dilution. Membrane staining was conducted at 4°C for 30 to 60 min, while recycling assays were performed at 37°C for indicated times. Slides were then rinsed in twice in 1× PBS, and fixed in 1% paraformaldehyde (PFA) prepared in PBS.

For penetrant staining, cells on coverslips were fixed in 4% PFA, permeabilized (0.02% Triton X-100 in PBS, 5 min), blocked in 5% BSA, incubated with primary and secondary antibodies separated by PBS washes, and mounted on glass slides with ProLong Diamond antifade reagent with DAPI (Invitrogen). Nuclear staining is depicted in blue, unless otherwise noted. Samples were imaged on a Leica DM6000 multiphoton confocal laser scanning microscope or a Leica DMIRE2 epifluorescence microscope. Images were colourized and composited in ImageJ software (National Institutes of Health; http://rsb.info.nih.gov/ij/), and assembled using Adobe Photoshop CS5. All microscopy presented in the manuscript is representative of a minimum of two biological replicates with several unique fields of view imaged and analysed therein.

An ImageJ plugin was used to evaluate protein colocalisation via van Steensel x-translation, which compares the Pearson's correlation coefficient obtained from the unmodified red and green signals (r_{obs} at $\Delta x=0$) with the pattern produced when one channel is shifted in the x-axis (r_{rand}, $\Delta x\neq0$). Correlation was considered significant when r generated from the actual observations, r_{obs}, exceeded the coefficient produced from multiple, randomized green-channel images, r_{rand}, at least 95% of the time. Cells that failed this stipulation were assigned an r_{obs} of 0 for the purposes of batch quantitation. A total of 41 x-translation iterations were performed.Mean cellular fluorescence was also measured in ImageJ by masking individual cells and determining the mean grey value in the region of interest (ROI).

All statistical analyses were performed in GraphPad Prism 7.0. Specific test details are provided in the figure legends.

Acknowledgements

We wish to thank Dr Michaela Strüder-Kypke for ongoing microscopy mentorship, Dr Jane McGlade for reagents, Sylvie Tremblay for initial Cbl biochemistry, and Ava Keyvani Chahi and Valmy Assam for ShcA molecular work.

Competing interests

The authors declare no competing or financial interests.

Author contributions

Conceptualization: M.K.B.W., N.J.; Methodology: M.K.B.W.; N. J. Validation: H.R.L.; Formal analysis: M.K.B.W.; N.J. Investigation: M.K.B.W., H.R.L., N.J.; Resources: N.J.; Writing - original draft: M.K.B.W.; Writing - review & editing: M.K.B.W., N.J.; Visualization: M.K.B.W.; Supervision: N.J.; Project administration: M.K.B.W.; N.J. Funding acquisition: N.J.

Funding

This work was supported by grants to N.J. from the Natural Sciences and Engineering Research Council of Canada (NSERC Discovery Grant RG327372) and the Brain Tumour Foundation of Canada. N.J. is recipient of an NSERC University Faculty Award and a Tier Two Canada Research Chair. H.R.L. received an NSERC CGS-M, and M.K.B.W. was awarded a Canadian Institutes of Health Research (CIHR) Vanier Canada Graduate Scholarship, and the University of Guelph Brock Doctoral Scholarship.

Supplementary information

Supplementary information available online at
http://jcs.biologists.org/lookup/doi/10.1242/jcs.198903.supplemental

References

Ahmed, S. B. M. and Prigent, S. A. (2014). A nuclear export signal and oxidative stress regulate ShcD subcellular localisation: a potential role for ShcD in the nucleus. *Cell. Signal.* **26**, 32-40.

Cai, Z., Zhang, H., Liu, J., Berezov, A., Murali, R., Wang, Q. and Greene, M. I. (2010). Targeting erbB receptors. *Semin. Cell Dev. Biol.* **9**, 1-6.

Carbone, R., Fre, S., Iannolo, G., Belleudi, F., Mancini, P., Pelicci, P. G., Torrisi, M. R. and Di Fiore, P. P. (1997). eps15 and eps15R are essential components of the endocytic pathway. *Cancer Res.* **57**, 5498-5504.

Chi, S., Cao, H., Wang, Y. and McNiven, M. A. (2011). Recycling of the epidermal growth factor receptor is mediated by a novel form of the clathrin adaptor protein Eps15. *J. Biol. Chem.* **286**, 35196-35208.

Chung, B. M., Raja, S. M., Clubb, R. J., Tu, C., George, M., Band, V. and Band, H. (2009). Aberrant trafficking of NSCLC-associated EGFR mutants through the endocytic recycling pathway promotes interaction with Src. *BMC Cell Biol.* **10**, 84.

Dinneen, J. L. and Ceresa, B. P. (2004). Continual expression of Rab5(Q79L) causes a ligand-independent EGFR internalization and diminishes EGFR activity. *Traffic* **5**, 606-615.

Fagiani, E., Giardina, G., Luzi, L., Cesaroni, M., Quarto, M., Capra, M., Germano, G., Bono, M., Capillo, M., Pelicci, P. et al. (2007). RaLP, a new member of the Src homology and collagen family, regulates cell migration and tumor growth of metastatic melanomas. *Cancer Res.* **67**, 3064-3073.

Fortian, A., Dionne, L. K., Hong, S. H., Kim, W., Gygi, S. P., Watkins, S. C. and Sorkin, A. (2015). Endocytosis of ubiquitylation-deficient EGFR mutants via clathrin-coated pits is mediated by ubiquitylation. *Traffic* **16**, 1137-1154.

Fukazawa, T., Miyake, S., Band, V. and Band, H. (1996). Tyrosine phosphorylation of Cbl upon epidermal growth factor (EGF) stimulation and its association with EGF receptor and downstream signaling proteins. *J. Biol. Chem.* **271**, 14554-14559.

George, R., Chan, H.-L., Ahmed, Z., Suen, K. M., Stevens, C. N., Levitt, J. A., Suhling, K., Timms, J. and Ladbury, J. E. (2009). A complex of Shc and RanGTPase localises to the cell nucleus. *Cell. Mol. Life Sci.* **66**, 711-720.

Goh, L. K. and Sorkin, A. (2013). Endocytosis of receptor tyrosine kinases. *Cold Spring Harbor Perspect. Biol.* **5**, a017459-a017459.

Grøvdal, L. M., Stang, E., Sorkin, A. and Madshus, I. H. (2004). Direct interaction of Cbl with pTyr 1045 of the EGF receptor (EGFR) is required to sort the EGFR to lysosomes for degradation. *Exp. Cell Res.* **300**, 388-395.

Han, W., Zhang, T., Yu, H., Foulke, J. G. and Tang, C. K. (2006). Hypophosphorylation of residue Y1045 leads to defective downregulation of EGFRvIII. *Cancer Biol. Ther.* **5**, 1361-1368.

Huang, F., Kirkpatrick, D., Jiang, X., Gygi, S. and Sorkin, A. (2006). Differential regulation of EGF receptor internalization and degradation by multiubiquitination within the kinase domain. *Mol. Cell* **21**, 737-748.

Jones, N., Hardy, W. R., Friese, M. B., Jorgensen, C., Smith, M. J., Woody, N. M., Burden, S. J. and Pawson, T. (2007). Analysis of a Shc family adaptor protein, ShcD/Shc4, that associates with muscle-specific kinase. *Mol. Cell. Biol.* **27**, 4759-4773.

Kazazic, M., Bertelsen, V., Pedersen, K. W., Vuong, T. T., Grandal, M. V., Rødland, M. S., Traub, L. M., Stang, E. and Madshus, I. H. (2009). Epsin 1 is involved in recruitment of ubiquitinated EGF receptors into clathrin-coated pits. *Traffic* **10**, 235-245.

Khan, E. M., Heidinger, J. M., Levy, M., Lisanti, M. P., Ravid, T. and Goldkorn, T. (2006). Epidermal growth factor receptor exposed to oxidative stress undergoes Src- and caveolin-1-dependent perinuclear trafficking. *J. Biol. Chem.* **281**, 14486-14493.

la Cour, T., Kiemer, L., Mølgaard, A., Gupta, R., Skriver, K. and Brunak, S. (2004). Analysis and prediction of leucine-rich nuclear export signals. *Protein Eng. Des. Sel.* **17**, 527-536.

McMahon, H. T. and Boucrot, E. (2011). Molecular mechanism and physiological functions of clathrin-mediated endocytosis. *Nat. Rev. Mol. Cell Biol.* **12**, 517-533.

Migliaccio, E., Mele, S., Salcini, A. E., Pelicci, G., Lai, K.-M. V., Superti-Furga, G., Pawson, T., Di Fiore, P. P., Lanfrancone, L. and Pelicci, P. G. (1997). Opposite effects of the p52shc/p46shc and p66shc splicing isoforms on the EGF receptor-MAP kinase-fos signalling pathway. *EMBO J.* **16**, 706-716.

Murphy, J. E., Padilla, B. E., Hasdemir, B., Cottrell, G. S. and Bunnett, N. W. (2009). Endosomes: a legitimate platform for the signaling train. *Proc. Natl Acad. Sci. USA* **106**, 17615-17622.

Nesterov, A., Carter, R. E., Sorkina, T. and Gill, G. N. (1999). Inhibition of the receptor-binding function of clathrin adaptor protein AP-2 by dominant-negative mutant μ2 subunit and its effects on endocytosis. *EMBO J.* **18**, 2489-2499.

Okabayashi, Y., Sugimoto, Y., Totty, N. F., Hsuan, J., Kido, Y., Sakaguchi, K., Gout, I., Waterfield, M. D. and Kasuga, M. (1996). Interaction of Shc with adaptor protein adaptins. *J. Biol. Chem.* **271**, 5265-5269.

Pols, M. S. and Klumperman, J. (2009). Trafficking and function of the tetraspanin CD63. *Exp. Cell Res.* **315**, 1584-1592.

Ravichandran, K. S., Zhou, M. M., Pratt, J. C., Harlan, J. E., Walk, S. F., Fesik, S. W. and Burakoff, S. J. (1997). Evidence for a requirement for both phospholipid and phosphotyrosine binding via the Shc phosphotyrosine-binding domain in vivo. *Mol. Cell. Biol.* **17**, 5540-5549.

Ravid, T., Sweeney, C., Gee, P., Carraway, K. L.,III and Goldkorn, T. (2002). Epidermal growth factor receptor activation under oxidative stress fails to promote c-Cbl mediated down-regulation. *J. Biol. Chem.* **277**, 31214-31219.

Rozakis-Adcock, M., McGlade, J., Mbamalu, G., Pelicci, G., Daly, R., Li, W., Batzer, A., Thomas, S., Brugge, J. and Pelicci, P. G. (1992). Association of the Shc and Grb2/Sem5 SH2-containing proteins is implicated in activation of the Ras pathway by tyrosine kinases. *Nature* **360**, 689-692.

Rush, J. S. and Ceresa, B. P. (2013). Molecular and cellular endocrinology. *Mol. Cell. Endocrinol.* **381**, 188-197.

Sakaguchi, K., Okabayashi, Y. and Kasuga, M. (2001). Shc mediates ligand-induced internalization of epidermal growth factor receptors. *Biochem. Biophys. Res. Commun.* **282**, 1154-1160.

Smith, C. J. and McGlade, C. J. (2014). The ubiquitin ligase RNF126 regulates the retrograde sorting of the cation-independent mannose 6-phosphate receptor. *Exp. Cell Res.* **320**, 219-232.

Sorkin, A. and Goh, L. K. (2009). Endocytosis and intracellular trafficking of ErbBs. *Exp. Cell Res.* **315**, 683-696.

Sorkin, A., Mazzotti, M., Sorkina, T., Scotto, L. and Beguinot, L. (1996). Epidermal growth factor receptor interaction with clathrin adaptors is mediated by the Tyr974-containing internalization motif. *J. Biol. Chem.* **271**, 13377-13384.

Tomas, A., Futter, C. E. and Eden, E. R. (2014). EGF receptor trafficking: consequences for signaling and cancer. *Trends Cell Biol.* **24**, 26-34.

Tong, J., Taylor, P. and Moran, M. F. (2014). Proteomic analysis of the epidermal growth factor receptor (EGFR) interactome and post-translational modifications associated with receptor endocytosis in response to EGF and stress. *Mol. Cell Proteomics* **13**, 1644-1658.

Umebayashi, K., Stenmark, H. and Yoshimori, T. (2008). Ubc4/5 and c-Cbl continue to ubiquitinate EGF receptor after internalization to facilitate polyubiquitination and degradation. *Mol. Biol. Cell* **19**, 3454-3462.

van der Geer, P., Wiley, S., Gish, G. D. and Pawson, T. (1996). The Shc adaptor protein is highly phosphorylated at conserved, twin tyrosine residues (Y239/240) that mediate protein-protein interactions. *Curr. Biol.* **6**, 1435-1444.

Wills, M. K. B. and Jones, N. (2012). Teaching an old dogma new tricks: twenty years of Shc adaptor signalling. *Biochem. J.* **447**, 1-16.

Wills, M. K. B., Tong, J., Tremblay, S. L., Moran, M. F. and Jones, N. (2014). The ShcD signaling adaptor facilitates ligand-independent phosphorylation of the EGF receptor. *Mol. Biol. Cell* **25**, 739-752.

Wills, M. K. B., Keyvani Chahi, A., Lau, H. R., Tilak, M., Guild, B., New, L. A., Lu, P., Jacquet, K., Meakin, S. O., Bisson, N. et al. (2017). Signaling adaptor ShcD suppresses extracellular signal-regulated kinase (Erk) phosphorylation distal to the Ret and Trk neurotrophic receptors. *J. Biol. Chem.* **292**, 5748-5759.

Yoshida, S., Masaki, T., Feng, H., Yuji, J., Miyauchi, Y., Funaki, T., Yoshiji, H., Matsumoto, K., Uchida, N., Watanabe, S. et al. (2004). Enhanced expression of adaptor molecule p46 Shc in nuclei of hepatocellular carcinoma cells: study of LEC rats. *Int. J. Oncol.* **25**, 1089-1096.

Yukimasa, S., Masaki, T., Yoshida, S., Uchida, N., Watanabe, S., Usuki, H., Yoshiji, H., Maeta, T., Ebara, K., Nakatsu, T. et al. (2005). Enhanced expression of p46 Shc in the nucleus and p52 Shc in the cytoplasm of human gastric cancer. *Int. J. Oncol.* **26**, 905-911.